

Constraining the flavor changing Higgs couplings to the top-quark at the LHC

David Atwood,^a Sudhir Kumar Gupta,^b and Amarjit Soni^c

^a*Dept. of Physics and Astronomy, Iowa State University,
Ames, IA 50011, USA*

^b*ARC Centre of Excellence for Particle Physics at the Terascale, School of Physics, Monash
University, Melbourne, Victoria 3800 Australia*

^c*Theory Group, Brookhaven National Laboratory,
Upton, NY, 11973, USA*

E-mail: atwood@iastate.edu, Sudhir.Gupta@monash.edu,
adlersoni@gmail.com

ABSTRACT: We study the flavor-changing couplings of the Higgs-boson with the top-quark using the processes: (a) $pp \rightarrow tt$, (b) $pp \rightarrow \bar{t}j$, and, (c) $pp \rightarrow \bar{t}jh$ at the LHC in light of current discovery of a 126 GeV Higgs-Boson. Sensitivities for the flavor-changing couplings are estimated using the LHC data that was collected until spring 2013. It is found that the process (c) is the most capable of yielding the best upper bound on the flavor-changing couplings with 2σ level sensitivities of $|\xi_{tc}^2 + \xi_{tu}^2|^{1/2} \lesssim 4.2 \times 10^{-3}$ and $\lesssim 1.7 \times 10^{-3}$ resulting from $t \rightarrow bl\nu_l$, $h \rightarrow jj$ with the 7 TeV and 8 TeV centre-of-mass energies respectively using existing data from the LHC. The corresponding bounds from $h \rightarrow b\bar{b}$ are worse by a factor of about 1.8.

Contents

1	Introduction	1
2	The flavor-changing top-quark couplings	2
3	Higgs boson and top-quark decay rates	3
3.1	Top quark decays	3
3.2	Decays of the Higgs-Boson	4
4	Production Processes at the LHC	4
5	Flavor-changing Higgs and LHC observations	7
5.1	Flavor changing couplings at the LHC-7 and LHC-8	7
5.2	Projected sensitivities at the LHC-14	12
6	Conclusions	13
A	Composition of $pp \rightarrow t\bar{q}_u(\bar{t}q_u)$ where $q_u = \{u, c\}$	15
A.1	For $\sqrt{s} = 7$ TeV	15
A.2	For $\sqrt{s} = 8$ TeV	15

1 Introduction

Last year the ATLAS and the CMS experiments at the LHC made a monumental discovery, namely that of a scalar resonance with mass of about 126 GeV and properties akin to that of a Standard Model (SM) Higgs boson [1, 2]. By now all of the prominent decay modes that have been measured are found to be quite consistent within appreciable errors with expectations based on the SM [3, 4].

Given that this particle is of such a fundamental importance it should be clear that we need to study all its properties to excruciating details. In particular, we have to understand the issue of its stability against radiative corrections. Naively, one expects new physics to be there around a few TeV scale. To decipher its nature we are likely to need very precise measurements of the couplings of the Higgs.

In this work we will address the flavor changing couplings involving the Higgs and the top-quark and try to use data to constrain these couplings. As is well known within the SM, such flavor off-diagonal couplings are highly suppressed and occur only at loop level. At least in some popular models, such as warped extra-dimension the Higgs and the top-quark may be particularly sensitive to flavor changing effects

as both of them are localized close to the TeV brane and the profiles of the KK-gluons are also peaked there [5–13]. We study several different processes involving the top-quark and the Higgs and find that $pp \rightarrow \bar{t}jh$, (where j is a jet), is very sensitive in providing stringent constraints.

In warped models of course there are also general expectations of extra CP violating phases of $\mathcal{O}(1)$. So CP violation studies are also highly motivated and we will return to this in another publication.

If such FCNCs are present, depending upon their size, they can influence the top-induced production processes, such as the single-top production processes where the top-quark is produced in association with lighter quarks, and Higgs, it can also modify (1) decay of the top-quark by allowing its decays into the Higgs-boson and a charm or an up-quark in addition to its known decays within the SM, and, (2) decay of the Higgs-boson into a virtual top-quark in association with a charm or an up-quark where the virtual top-decays as in (1).

The organisation of the paper is following: We begin with a brief introduction to the flavor-changing operators. In Sections 3 and 4 we will discuss decays of the Higgs boson and the top-quark, and the production processes we propose in this article. In section 5 we will present the actual analysis of the proposed processes in the light of LHC data on the Higgs-boson and the pre-existing data on the top-quark from the Tevatron experiment. Finally we summarise our findings in Section 6.

2 The flavor-changing top-quark couplings

When the flavor-changing couplings of the Higgs are present, the SM Lagrangian can be extended by allowing the following additional terms,

$$\mathcal{L}_{flavor}^h = \xi_{tc}\bar{t}cH + \xi_{tu}\bar{t}uH + h.c., \quad (2.1)$$

where for now, we consider that the flavor-changing couplings, ξ_{tu} , and, ξ_{tc} are real and symmetric, i. e. $\xi_{tq_u} = \xi_{tq_u}^\dagger = \xi_{q_u t} = \xi_{q_u t}^\dagger$, where, $q_u = u, c$. As mentioned before, CP studies will be dealt with in a later study.

It is to be noted here that similar flavor-changing Lagrangian has been also widely studied in the Refs. [14–20], for example. These FV-interactions allow some interesting phenomenological consequences which are as follows:

(A) *At the decay level*

1. In addition to the usual decay modes, Higgs can also decay into single W^\pm -boson via an off-shell top, e.g. $h \rightarrow \bar{q}_u(t^* \rightarrow bW^+)$; ($q_u = u, c$) where ‘*’ means off-shell top,

2. top-quark can now also decay into a charm or an up-quark and a Higgs, e.g. $t \rightarrow q_u h$.

(B) *At the production level*

1. Because of FCNC we can have a pair of same-sign top produced via t-channel exchange of the Higgs, e.g. $pp \rightarrow tt(\bar{t}\bar{t})$ through the parton level subprocesses, $uu \rightarrow tt$, $uc \rightarrow tt$ and $cc \rightarrow tt$.

2. The FCNCs of Higgs can contribute significantly to the production processes where a top-quark is produced in association with light partons, e.g. $pp \rightarrow t\bar{j}_u(\bar{t}j_u)$, where $j_u = u, c$.

3. Higgs can now be produced in association with a top-quark and an up or a charm quark, e.g. the process $pp \rightarrow t\bar{c}h(\bar{t}ch)$.

Let us discuss their consequences one-by-one in the following sections.

3 Higgs boson and top-quark decay rates

Let us now consider the decays of top-quark and Higgs-boson in the following subsections:

3.1 Top quark decays

Because $m_t - m_h > m_c, m_u, m_b$, in addition to the usual decay into a bottom quark and a W^+ Boson, the top-quark can also decay into a charm (or an up) quark and a Higgs-Boson. Therefore, the total decay width of the top-quark, Γ_t will take the following form,

$$\Gamma_t = \Gamma_{t \rightarrow bW^+} + \Gamma_{t \rightarrow ch} + \Gamma_{t \rightarrow uh}. \quad (3.1)$$

The $t \rightarrow bW^+$ decay width at the NLO level is given by [21, 22],

$$\Gamma_{t \rightarrow bW^+} = \frac{G_F m_t^3}{8\sqrt{2}\pi} \left[1 - \frac{2\alpha_s}{3\pi} \left(\frac{2\pi^2}{3} - \frac{5}{2} \right) \right] (1 - \tau_W^2)^2 (2\tau_W^2 + 1) \quad (3.2)$$

The $t \rightarrow q_u h$ ($q_u = u, c$) partial decay width is given as,

$$\Gamma_{t \rightarrow q_u h} = \frac{\xi_{tq_u}^2 m_t}{16\pi} [(\tau_{q_u} + 1)^2 - \tau_h^2] \sqrt{1 - (\tau_h - \tau_{q_u})^2} \sqrt{1 - (\tau_{q_u} + \tau_h)^2} \quad (3.3)$$

where, $\tau_W = \frac{M_W}{m_t}$, $\tau_h = \frac{M_h}{m_t}$, $\tau_{q_h} = \frac{m_{q_h}}{m_t}$. Using the measured values of G_F , α_s , M_W , M_h etc., we obtain,

$$\Gamma_t = \Gamma_t^{SM} + [0.8 \xi_{tc}^2 + 0.78 \xi_{tu}^2] \text{ GeV}, \quad (3.4)$$

where $\Gamma_t^{SM} = 2 \pm 0.7 \text{ GeV}$ [22] and $\Gamma_t^{SM} \equiv \Gamma_{t \rightarrow bW^+}^{SM}$.

From the above expression it is clear that the maximum deviation in the $Br(t \rightarrow bW^+)$ from the SM corresponds to the $\xi_{tc} = 1 = \xi_{tu}$ and amounts to be about 41%. As we will show later in this paper, the current LHC data constraints on these FCNCs will be much stronger, i. e. $\lesssim 10^{-3}$. To put things into perspective, in the SM, the diagonal couplings of the top-quark and the charm-quark $y_{t,c} = \frac{\sqrt{2}m_{t,c}}{v}$; $v = 246$ GeV being the vacuum-expectation value, are $y_t \simeq 1$ and $y_c \simeq 0.008$ respectively.

3.2 Decays of the Higgs-Boson

Because of the flavor-changing couplings endowed by Eqn. (2.1) the Higgs-Boson can also have the following three-body decays:

$h \rightarrow q_u(\bar{t}^* \rightarrow \bar{b}W^-)$, $h \rightarrow \bar{q}_u(t^* \rightarrow bW^+)$; ($q_u = u, c$) where “*” means off-shell top. Using CalcHep [23] we numerically estimate,

$$\Gamma_{h \rightarrow q_u(\bar{t}^* \rightarrow \bar{b}W^-)} \simeq 0.28 \xi_{tq_u}^2 \text{ MeV}. \quad (3.5)$$

Therefore the total width, Γ_h would be,

$$\begin{aligned} \Gamma_h &= \Gamma_h^{SM} + \sum_{q_u} \Gamma_{h \rightarrow q_u(\bar{t}^* \rightarrow \bar{b}W^-)} + \Gamma_{h \rightarrow \bar{q}_u(t^* \rightarrow bW^+)} \\ &\simeq [\Gamma_h^{SM} + 0.56 (\xi_{tc}^2 + \xi_{tu}^2)] \text{ MeV}, \end{aligned} \quad (3.6)$$

where $\Gamma_h^{SM} = 3.3$ using CalcHep.

In our model the usual two-body decays of the Higgs boson, i.e., the LHC Higgs observables would take the following form,

$$\mathcal{R}_{ggX} = \frac{\sigma_{gg \rightarrow h}}{\sigma_{gg \rightarrow h}^{SM}} \cdot \frac{\mathcal{BR}(h \rightarrow X)}{\mathcal{BR}^{SM}(h \rightarrow X)} \simeq \frac{\Gamma_{h \rightarrow gg}}{\Gamma_{h \rightarrow gg}^{SM}} \cdot \left(\frac{\Gamma_{h \rightarrow X}}{\Gamma_h} \right) / \left(\frac{\Gamma_{h \rightarrow X}^{SM}}{\Gamma_h^{SM}} \right) \simeq \frac{\Gamma_h^{SM}}{\Gamma_h}; \quad (3.7)$$

where, X stands for two-body decay products of the produced Higgs-Boson, e.g. $X = \gamma\gamma, b\bar{b}, WW^*, ZZ^*, \tau^+\tau^-$ etc. In the equation above, we have assumed that $\frac{\sigma_{gg \rightarrow h}}{\sigma_{gg \rightarrow h}^{SM}} = \frac{\Gamma_{gg \rightarrow h}}{\Gamma_{gg \rightarrow h}^{SM}} \simeq 1$ which is due to the fact that the flavor-changing couplings discussed in our paper affect the $gg \rightarrow h$ production process at the next-loop level and therefore the effects are expected to be much smaller.

4 Production Processes at the LHC

We now turn to study some interesting production processes where the effect of the aforementioned flavor-changing couplings could be significant. Obviously the very first process, the $t\bar{t}$ may not be suitable when both the produced tops decay through their usual SM decay model as it will have relatively large SM background. Among the other leading processes are:

- (a) the same-sign top-pair, e.g. $pp \rightarrow tt(\bar{t}\bar{t})$,
- (b) processes where a top-quark is produced in association with a light jet, e.g. $pp \rightarrow t\bar{j}_u(\bar{t}j_u)$, where $j_u = u, c$, and,
- (c) processes where the top-quark is produced in association with a Higgs and a light jet, e.g. $pp \rightarrow t\bar{j}_uh(\bar{t}j_uh)$.

The process (a), the same-sign top pair production is an interesting one as it has very little SM background. In a recent work by us [24], it was found that this process can play a very important role in excluding many models proposed to explain the forward-backward asymmetry of the top-quark A_{FB}^t as observed by the Tevatron experiments (Also see, for example, [25–27]). Within the model under consideration in this paper, at the LHC, a pair of same-sign top pair can be produced via the t-channel exchange of the Higgs through two flavor-changing couplings. For the $m_h = 125.7$ GeV, the bare cross-sections for this process is given by the following equations:

$$\begin{aligned}\sigma(pp \rightarrow tt) &= 49.5\xi_{tu}^4 + 13.6\xi_{tc}^2\xi_{tu}^2 + 0.3\xi_{tc}^4 \text{ pb (at } \sqrt{s} = 7 \text{ TeV)}, \\ \sigma(pp \rightarrow tt) &= 56.2\xi_{tu}^4 + 17.7\xi_{tc}^2\xi_{tu}^2 + 0.4\xi_{tc}^4 \text{ pb (at } \sqrt{s} = 8 \text{ TeV)},\end{aligned}\quad (4.1)$$

respectively.

In Eqns. above we notice that the numerical factors for the ξ_{tu}^4 is larger than those proportional to $\xi_{tc}^2\xi_{tu}^2$ and ξ_{tc}^4 . This is because of the fact that the first term is due to the scattering of two valence up-quarks as opposed to other terms where one or both the initial partons are the (sea-)charm-quark(s). As discussed in Refs. [24] and in [28] this process has very little SM background and hence can be useful in constraining the couplings ξ_{tc} and ξ_{tu} . We will discuss this in detail in a later section.

The other two processes namely, (b) and (c) are perhaps even more interesting as both of these occur via only one flavor-changing vertex unlike the process (a). Therefore, we expect the cross-sections for these processes to be proportional to $a\xi_{tu}^2 + b\xi_{tc}^2$ where a and b are arbitrary constants.

More specifically, the processes where a top or anti-top quark is produced in association with an up, anti-up, charm or anti-charm quark can occur via two ways: one, where a pair of initial (anti-)quarks with same or different flavor undergo t-channel exchange through the Higgs, e.g. processes of the form $qq_u \rightarrow tq$ and $q\bar{q}_u \rightarrow \bar{t}q$, where, $q = \{q_u, b\}$, $q_u = \{u, c\}$. Therefore we expect cross-sections for these subprocesses to be proportional to $y_q^2\xi_{tq_u}^2$ where y_q is the Yukawa coupling of the quark q. This suggests that although at the subprocess

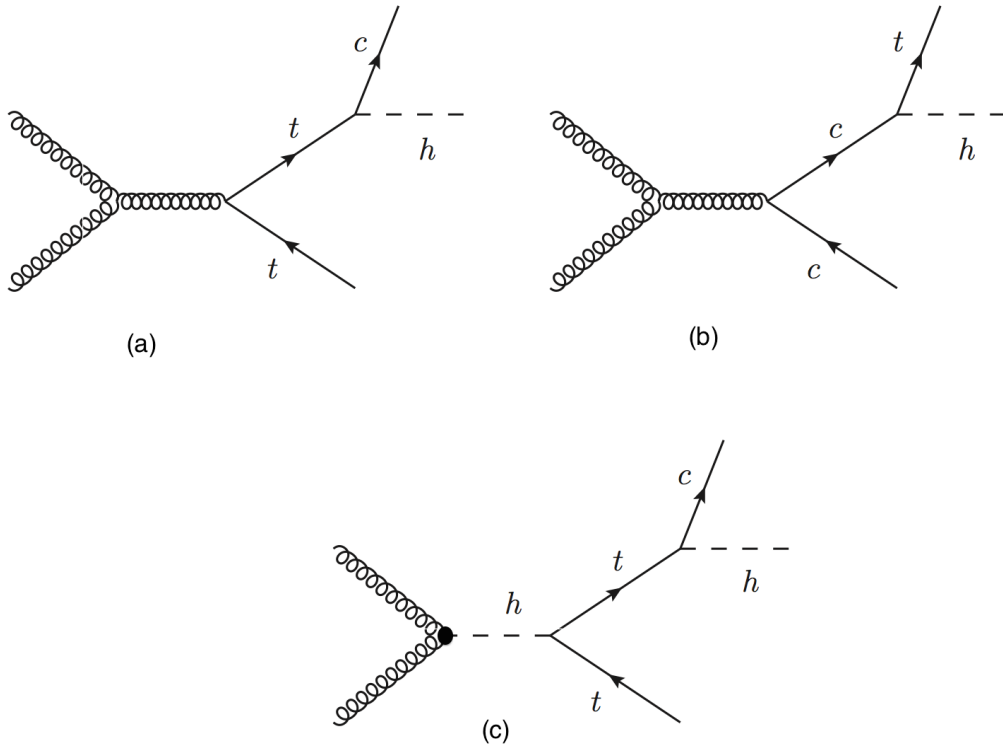


Figure 1: Representative s-channel Feynman diagrams for the partonic process $gg \rightarrow tch$.

level, we gain in the processes where the initial parton is a b or a \bar{b} due to large value of y_b compared to y_c and y_u at the proton-proton level, we may lose due to relatively smaller parton densities for the b -quarks. The other type of contribution is due to the off-shell Higgs production in the s-channel due to gluon-pair fusion, where the Higgs decays into $t\bar{q}_u$ or $\bar{t}q_u$. The composition of this process is discussed in detail for $m_h = 125.7$ GeV in the Appendix A. The corresponding background and the total cross-sections for $\sqrt{s} = 7$ and 8 TeV are summarised in Table 1. The major source for this process is production of $t\bar{b}(\bar{t}b)$ mediated by an off-shell W^\pm in the s-channel.

The production process (c) requires production of a $t\bar{t}$ pair where one of the top decays into a Higgs and an up or charm-quark, or it can also take place via the pair production processes $u\bar{u}$ and $c\bar{c}$ where one of the off-shell up or charm goes into a top and a Higgs (see Fig 1). This process has very little SM background due to the production of (i) $t\bar{b}Z(\bar{t}bZ)$, and, (ii) $t\bar{b}h(\bar{t}bh)$. Clearly both of these processes are electro-weak processes which are mediated by an off-shell W^\pm -boson. e.g., $pp \rightarrow W^{\pm*}Z(W^{\pm*}h)$, and $W^* \rightarrow t\bar{b}(\bar{t}b)$. Therefore we expect to find better bounds on ξ_{tc} and ξ_{tu} using this process. A detail of the cross-sections and corresponding background to this process is given in Table 2.

Serial Number	Process	LHC-7	LHC-8
(1)	$pp \rightarrow t\bar{c}(\bar{t}c, tc, \bar{t}\bar{c})$	$42.06\xi_{tc}^2 + 4.81\xi_{tu}^2$	$59.7\xi_{tc}^2 + 5.44\xi_{tu}^2$
(2)	$pp \rightarrow h \rightarrow t\bar{c}(\bar{t}c)$	$41.2\xi_{tc}^2$	$58.52\xi_{tc}^2$
(3)	$pp \rightarrow t\bar{u}(\bar{t}u, tu, \bar{t}\bar{u})$	$0.4\xi_{tc}^2 + 44.54\xi_{tu}^2$	$0.61\xi_{tc}^2 + 59.67\xi_{tu}^2$
(4)	$pp \rightarrow h \rightarrow t\bar{u}(\bar{t}u)$	$41.2\xi_{tu}^2$	$58.52\xi_{tu}^2$
(1) + (3)	$pp \rightarrow tq_u(\bar{t}q_u)$	$42.46\xi_{tc}^2 + 49.35\xi_{tu}^2$	$60.31\xi_{tc}^2 + 65.11\xi_{tu}^2$
SM Background	$pp \rightarrow t\bar{b}(\bar{t}b, tj, \bar{t}j, tjj, \bar{t}jj)$	43.49×10^3	56.17×10^3

Table 1: Single top production cross-section (in fb units) at the LHC for $\sqrt{s} = 7$ and 8 TeV in association with an up or a charm (anti-)quark. In all the processes the implemented basic cuts on the associated (anti-)quark are as follows: $p_T = 25$ GeV, and, $|\eta| \leq 2.7$. The Yuwaka couplings y_u, y_c, y_t have been estimated using $m_u = 3$ MeV, $m_c = 1.44$ GeV and $m_t = 172.4$ GeV respectively. The Higgs-Boson mass has been set to the observed central value, $m_h = 125.7$ GeV.

Serial Number	Process	LHC-7	LHC-8
(5)	$pp \rightarrow t\bar{c}h(\bar{t}ch, tch, \bar{t}\bar{c}h)$	$75.25 \times 10^3 \xi_{tc}^2$	$107.99 \times 10^3 \xi_{tc}^2$
(6)	$pp \rightarrow t\bar{u}h(\bar{t}uh, tuh, \bar{t}\bar{u}h)$	$79.21 \times 10^3 \xi_{tu}^2$	$112.76 \times 10^3 \xi_{tu}^2$
(5) + (6)	$pp \rightarrow t\bar{q}_uh(\bar{t}q_uh)$	$(75.25\xi_{tc}^2 + 79.21\xi_{tu}^2) \times 10^3$	$(107.99\xi_{tc}^2 + 112.76\xi_{tu}^2) \times 10^3$
SM Background	$pp \rightarrow t\bar{b}Z(\bar{t}bZ)$	2.54 (1.07)	3.32 (1.39)
	$pp \rightarrow t\bar{t} + nj; n \leq 3$	176.6×10^3	261.5×10^3
	$pp \rightarrow t\bar{t} + b\bar{b} + nj; n \leq 3$	716.9	1175.6
	$pp \rightarrow t\bar{b}h(\bar{t}bh)$	0.54 (0.23)	0.7 (0.29)

Table 2: Single top production cross-section (in fb units) at the LHC for $\sqrt{s} = 7$ and 8 TeV in association with an up or a charm (anti-)quark and a Higgs-Boson. In all the processes the implemented basic cuts and all other SM parameters are same as given in Table 1.

5 Flavor-changing Higgs and LHC observations

In this Section we will first discuss the flavor-changing couplings ξ_{tc} and ξ_{tu} in the context of the individual experimental observations as listed in Table 3 and later we will make use of them all in order to obtain constraints on these couplings using the processes we propose here. We will also discuss the projected sensitivities of the aforementioned couplings in the context of 14 TeV data in the second Subsection.

5.1 Flavor changing couplings at the LHC-7 and LHC-8

Let us first begin with total decay width of the top-quark, Γ_t . As we have already noticed in Section 3.1, Γ_t receives positive contributions proportional to ξ_{tu}^2 and to ξ_{tc}^2 due to additional decay processes $t \rightarrow uh$ and $t \rightarrow ch$ respectively.

This gives an upper bound on the $\sqrt{\xi_{tc}^2 + \xi_{tu}^2}$ of about 1.3 at the 2σ level which is quite mild.

Observable	Value	Experiment
Γ_t	2 ± 0.7 GeV	Tevatron [22]
m_h	125.5 ± 0.2 (stat) $^{+0.5}_{-0.6}$ (sys) GeV 125.8 ± 0.5 (stat) ± 0.2 (sys) GeV 125.7 ± 0.4 GeV	ATLAS [3] CMS [4] Combined
$\mathcal{R}_{gg\gamma\gamma}$	$1.65^{+0.34}_{-0.30}$ $1.11^{+0.32}_{-0.30}$ 1.36 ± 0.23	ATLAS [29, 30] CMS [31, 32] Combined
$\mathcal{R}_{gg2l2\nu}$	1.01 ± 0.31 $0.76^{+0.21}_{-0.21}$ 0.84 ± 0.17	ATLAS [33, 34] CMS [35, 36] Combined
\mathcal{R}_{gg4l}	$1.7^{+0.5}_{-0.4}$ $0.91^{+0.30}_{-0.24}$ 1.12 ± 0.26	ATLAS [29, 37] CMS [35, 38] Combined
$D0$ -oscillations	$ \xi_{tu}\xi_{tc} < 0.9 \times 10^{-3}$	UTfit Collaboration [39]

Table 3: Measured values of various observables used in our analysis; combined here means weighted average of ATLAS and CMS values for a given observable.

In a similar way we study the Higgs observables $\mathcal{R}_{gg\gamma\gamma}$, $\mathcal{R}_{gg2l2\nu}$, \mathcal{R}_{gg4l} and their combined effects in light of recently updated data during Moriond-2013 as discussed in Table 3. Using the LHC data on various Higgs-observables, one obtains upper bounds on $\sqrt{\xi_{tc}^2 + \xi_{tu}^2}$ of about 1.7, 3.3, 1.8, and, 1.2, for $\mathcal{R}_{gg\gamma\gamma}$, $\mathcal{R}_{gg2l2\nu}$, \mathcal{R}_{gg4l} and for their combined effect respectively. This means the whole range of ξ_{tc} and ξ_{tu} (between -1 to +1) is allowed by these observables at the 2σ level. Note also that the bound that we will obtain later in this paper from $pp \rightarrow tch$ will be much stronger, $\lesssim 10^{-3}$.

In order to study the production processes we incorporated flavor-changing couplings in MadGraph5 [40]. We evaluate parton densities at a scale $\mu_R = \sqrt{\hat{s}} = \mu_F$ using CTEQ6L1 [41].

We present our result for the $\sqrt{s} = 7$ TeV with an integrated luminosity of $\int \mathcal{L} dt = 5 \text{ fb}^{-1}$ and for $\sqrt{s} = 8$ TeV with $\int \mathcal{L} dt = 22 \text{ fb}^{-1}$ in Figures 2 at the bare production level.

Using the formulae for the production cross-sections in our model and their respective SM backgrounds as mentioned in Eqns. 4.1 and Tables 1 and 2, and the constraints due to the Γ_t and the LHC Higgs discovery observables $\mathcal{R}_{gg\gamma\gamma}$, $\mathcal{R}_{gg2l2\nu}$, and, \mathcal{R}_{gg4l} , we find the following upper bounds on the $\sqrt{\xi_{tc}^2 + \xi_{tu}^2}$ at the 2σ level;

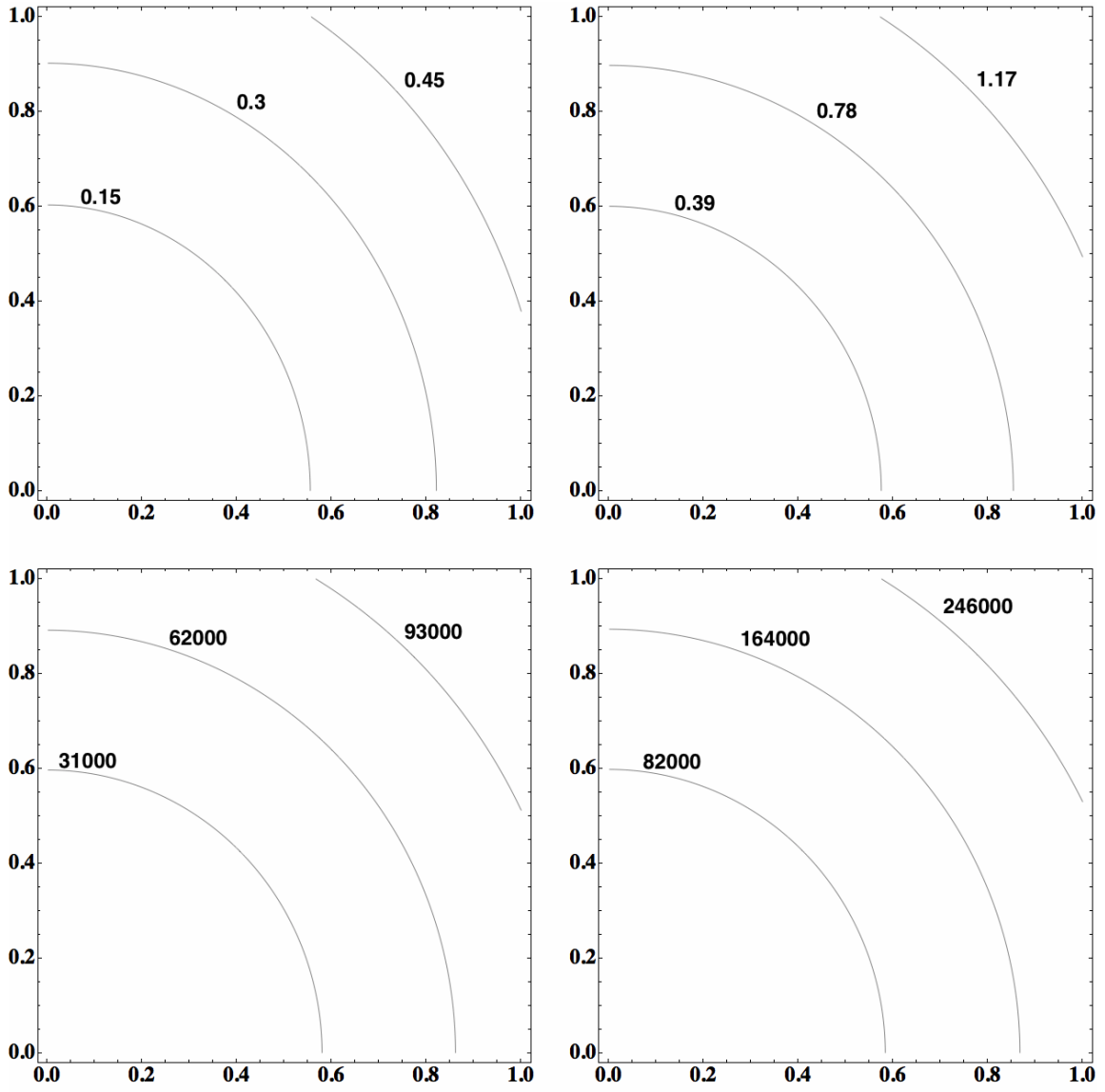


Figure 2: Contour plots in $\xi_{tc} - \xi_{tu}$ plane for signal-significance, $\frac{S}{\sqrt{B}}$, at the production level, for the processes $pp \rightarrow t\bar{j}_u(\bar{t}j_u)$ (top) and $pp \rightarrow t\bar{j}_uh(\bar{t}j_uh)$ (bottom) for $\sqrt{s} = 7$ (left) and 8 TeV (right) data at the LHC.

$$\sqrt{\xi_{tc}^2 + \xi_{tu}^2} \lesssim \begin{cases} 0.3 \text{ (0.17)} & \text{for process (a)} \\ 0.9 \text{ (0.9)} & \text{for process (b)} \\ 1.6 \text{ (0.6)} \times 10^{-3} & \text{for process (c)} \end{cases} . \quad (5.1)$$

for the $\sqrt{s} = 7$ TeV with 5 fb^{-1} ($\sqrt{s} = 8$ TeV with 22 fb^{-1}) data.

Clearly the bounds due to process (b) are not so promising which is partially due to the fact that it suffers from large SM background as mentioned in

Table 1. The reason for them being the same for both the 7 TeV and 8 TeV LHC centre-of-mass energies is that it in determining these the combined effect of the constraints on the top-quark decay width and the Higgs observables play a dominant role. Note also that although the processes (a) puts mild bound on $\sqrt{\xi_{tc}^2 + \xi_{tu}^2}$ it is interesting to analyse because it leads to unique signature in the form of a pair of same-sign leptons. The process (c) is certainly the best process among all of the aforementioned ones as it turns out to be very sensitive even to small values of the flavor-changing couplings.

It is to be noted that in order to obtain the aforementioned bounds, we have assumed that, (1) we will be able to reconstruct the produced (anti-)top-quark(s), and the Higgs boson fully in all its detection modes, and, (2) the number of signal events do not exceed one where the SM background is not significant for the given LHC luminosity. However due to poor reconstruction especially for the cases where the top-quark(s) decays hadronically into a b-jet and a pair of light parton jet, the above limits may not be so realistic. We therefore turn our focus to obtain the detection level bounds on these couplings. For this we work with processes with at least one lepton in the final state. Thus, in all the production processes we allow the produced (anti)top-quark to decay semileptonically, e.g. $t \rightarrow bl\nu_l$, where $l = e, \mu$. In case of the process (c) where a Higgs is also produced in association with the top-quark and a jet, we work with $h \rightarrow b\bar{b}$, $h \rightarrow \gamma\gamma$ and $h \rightarrow jj$, where $j = g, q, \bar{q}, b, \bar{b}$. The reason for considering $h \rightarrow b\bar{b}$ is merely to gain statistical advantage as within SM the branching ratio for $h \rightarrow b\bar{b}$ for the given value of m_h is about 79%. For the case where the Higgs decays into a pair of photons, although the branching ratio is quite suppressed $\simeq 2.9 \times 10^{-3}$, we expect it to be relatively cleaner than the $h \rightarrow b\bar{b}$ case.

With this in mind we will therefore have the following topologies:

- $l^\pm l^\pm + 2b - jets + \cancel{E}_T$, from the process (a),
- $l^\pm + j + b - jet + \cancel{E}_T$, from process (b), and,
- $l^\pm + j + 3b - jets + \cancel{E}_T$, when $h \rightarrow b\bar{b}$, $l^\pm + j + b - jet + 2\gamma + \cancel{E}_T$, when $h \rightarrow \gamma\gamma$, and, $l^\pm + 3j + b - jet + \cancel{E}_T$, when $h \rightarrow jj$, from process (c).

The set of basic cuts used on the photons/leptons/jets in our study are as follows:

$p_{T_{l,j,\gamma}} > 25$ GeV, $|\eta_{l,j,\gamma}| < 2.7$, $\Delta R_{kk}, \Delta R_{ik}, > 0.4$, $\cancel{E}_T > 30$ GeV, with $i, k = \{l, j, \gamma\}$. In addition, we also assume a b-jet identification efficiency of 58% [42].

Other SM Backgrounds: It is to be noted that because a light parton jet can fake the b-jet with probabilities of about 10% for a charm-jet and about 1%

Process	LHC-7	LHC-8
$pp \rightarrow t\bar{t} + n - jets$	176.64	261.52
$pp \rightarrow t\bar{t} + b\bar{b} + n - jets$	0.72	1.18
Total	177.36	262.7

Table 4: Other subleading SM backgrounds (in pb) for the production process (c) for $\sqrt{s} = 7$ and 8 TeV.

Process	LHC-7	LHC-8
$pp \rightarrow t\bar{t} + n - jets$	0.33	0.49
$pp \rightarrow t\bar{t} + b\bar{b} + n - jets$	0.0014	0.002
Total	0.33	0.49

Table 5: Other subleading SM backgrounds (in pb) for the production process (c) followed by the decays $h \rightarrow b\bar{b}$ and $t \rightarrow bl\nu_l$ for $\sqrt{s} = 7$ and 8 TeV.

for other light jets respectively [43]), there can be other subleading SM backgrounds for the process (c), particularly when $h \rightarrow b\bar{b}$ and $t \rightarrow bl\nu_l$. In this category, the leading background contribution comes from the processes $pp \rightarrow t\bar{t} + n - jets$ and $pp \rightarrow t\bar{t} + b\bar{b} + n - jets$, where n represents number of jets.¹

Using MadGraph, for $n \leq 3$, cross-sections for these processes have been estimated to be $\simeq 177$ pb and $\simeq 0.7$ pb respectively at the $\sqrt{s} = 7$ TeV at the bare level. With the above sets of basic cuts, for our final state $pp \rightarrow l^\pm + j + 3b - jets + \cancel{E}_T$, the requirement that one of the jet pair reconstructs to m_h within 2σ , these aforementioned backgrounds are reduced to 0.33 fb and 0.0014 fb respectively. The corresponding signal rates are reduced by 0.42, 0.57 and 0.43 respectively for the processes $l^\pm + j + 3b - jets + \cancel{E}_T$, $l^\pm + j + b - jet + 2\gamma + \cancel{E}_T$, and, $l^\pm + 3j + b - jet + \cancel{E}_T$. Similar estimates for $\sqrt{s} = 8$ TeV have been summarised in Table 4 and 5. Thus our estimates suggest that although at the production level such backgrounds are huge for the LHC integrated luminosities we consider in our analysis, with the aforementioned cuts, these can be reduced to a level where their effects become insignificant for our purposes.

Thus, after combining all the constraints from the Higgs observations and the top-quark decay width, one obtains the following 2σ bounds:

¹We thank J. Evans for discussion on this background.

$$\sqrt{\xi_{tc}^2 + \xi_{tu}^2} \lesssim \begin{cases} 0.6 \text{ (0.3)} & \text{for } pp \rightarrow l^\pm l^\pm + 2b - jets + \cancel{E}_T \\ 0.9 \text{ (0.9)} & \text{for } pp \rightarrow l^\pm + j + b - jet + \cancel{E}_T \\ 7.5 \text{ (2.9)} \times 10^{-3} & \text{for } pp \rightarrow l^\pm + j + 3b - jets + \cancel{E}_T \\ 11.9 \text{ (4.8)} \times 10^{-2} & \text{for } pp \rightarrow l^\pm + j + b - jet + 2\gamma + \cancel{E}_T \\ 4.2 \text{ (1.7)} \times 10^{-3} & \text{for } pp \rightarrow l^\pm + 3j + b - jet + \cancel{E}_T \end{cases} \quad (5.2)$$

for the $\sqrt{s} = 7$ TeV with 5 fb^{-1} ($\sqrt{s} = 8$ TeV with 22 fb^{-1}) data. Clearly the process $pp \rightarrow l^\pm + 3j + b - jet + \cancel{E}_T$ gives the best bound which is about $\mathcal{O}(1.7 \times 10^{-3})$ using the full 8 TeV data while the corresponding bound for the process $pp \rightarrow l^\pm + j + b - jet + 2\gamma + \cancel{E}_T$ is about $\mathcal{O}(4.8 \times 10^{-2})$ or so. A detailed list of sensitivities to all of these processes at individual and combined level is also presented in Table 6 for convenience. The corresponding bound on $t \rightarrow ch$ as reported in Ref. [19] and by the ATLAS [43] and CMS [44] experiments are about 0.1 which is about one order of magnitude larger than the best bound obtained by us. This is partially due to the fact that in obtaining tch final state we do not restrict ourselves merely to the pair-production of $t\bar{t}$ unlike them. Thus in their study only diagrams of type Figs. 1 (a) and 1 (c) are relevant; in our case all three processes in Fig 1 occur. This translates into about 14 times larger cross-section for us compared to $\sigma_{t\bar{t}} \times 2Br(t \rightarrow ch)$ as in their work too, the other top decays semileptonically as $t \rightarrow bl\nu_l$. Obviously, since in our case, one of the top-quarks decaying to ch or uh , can be off-shell, it results in a further advantage for us in terms of reconstruction efficiencies.

5.2 Projected sensitivities at the LHC-14

Guided with the aforementioned bounds as obtained from various final state topologies using the observed 7 and 8 TeV LHC data in the previous subsection, in this subsection we provide estimate for the forthcoming LHC run with $\sqrt{s} = 14$ TeV. As we have noticed above, the best bound on the $\sqrt{\xi_{tc}^2 + \xi_{tu}^2}$ correspond to the $pp \rightarrow l^\pm + 3j + b - jet + \cancel{E}_T$ detection mode. We will therefore focus on this particular detection mode itself.

Using MadGraph5, we find the bare cross-section for the production-process responsible for the aforementioned topology, $pp \rightarrow tch$, at $\sqrt{s} = 14$ TeV to be $431.5\xi_{tc}^2 + 441.2\xi_{tu}^2$ pb, which is about a factor of 4 larger compared to at 8 TeV, see Table 2. This in the ideal case assuming a full reconstruction of the tch and in the absence of any SM background yields, $\sqrt{\xi_{tc}^2 + \xi_{tu}^2} \lesssim 0.15 \times 10^{-3}$ for an integrated luminosity 100 fb^{-1} .

The cross-sections for the relevant SM processes which contribute to the background to our final-state are estimated to be, 6.01 (2.91) fb, 1.29 (0.59) fb,

and, 1161.3 pb for $pp \rightarrow t\bar{b}Z(\bar{t}bZ)$, $pp \rightarrow t\bar{b}h(\bar{t}bh)$, and, $pp \rightarrow t\bar{t} + nj; n \leq 3$ respectively. This, using the exact same cuts as mentioned in the previous subsection, and, the demand that the two jets reconstruct to a Higgs-Boson, and, the only lepton in our final state reconstruct to a top-quark when paired with the b-jet and the missing transverse energy, in our final state, translates into a net SM background of 2.18 fb for the final state under consideration. Thus from our complete analysis, we obtain $\sqrt{\xi_{tc}^2 + \xi_{tu}^2} \lesssim 1.39 (1.06) \times 10^{-3}$ for $\int \mathcal{L} dt = 100 (300) \text{ fb}^{-1}$. It is to be noted that this is better only by a factor of about 1.6 compared to the bound obtained using the 8 TeV data for the same signatures, while one naively expect it to be better by a factor of four. The reason behind this is that for 7 and 8 TeV data, the SM background was not so significant and therefore the criterion that the number of observed signal events should not exceed one turn out to be stronger while for 14 TeV case it was actually S/\sqrt{B} criterion which ruled over the former in estimating projected LHC sensitivities on the FCNC couplings.

6 Conclusions

We have studied the flavor-changing couplings of the Higgs boson with the top-quark in light of the Higgs discovery, using the data at the LHC, for both $\sqrt{s} = 7 \text{ TeV}$ and 8 TeV , along with the Tevatron measurements of the total decay width of the top-quark. In order to obtain better bounds to these processes we studied the same-sign top pair production, $pp \rightarrow tt(\bar{t}\bar{t})$, single top production in association with a light parton jet, $pp \rightarrow t\bar{j}(\bar{t}j)$, and the process where the single top-quark is produced in association with a Higgs and a light parton jet, $pp \rightarrow t\bar{j}h(\bar{t}jh)$. In our study, we found that the process $pp \rightarrow t\bar{j}h(\bar{t}jh)$ can be extremely useful in providing stronger bounds on the flavor-changing couplings of the order of 1.7×10^{-3} , particularly in case of the latter process with the Higgs-boson decays into a pair of jets and the (anti)top-quark decays semileptonically into a b-jet, a lepton and an invisible neutrino using the full data at $\sqrt{s} = 8 \text{ TeV}$. To put things in perspective, we mention in passing that these constraints are significantly better than the one obtained from top decays, following pair production of tops, and also single top production [45]. Our sensitivities on $\sqrt{\xi_{tc}^2 + \xi_{tu}^2}$ are complementary to the one obtained by the low energy experiments through the D0-oscillations [45] on the product $|\xi_{tc}\xi_{tu}|$ as listed in Table 3. Note that the latter product alone is not sufficient particularly when one of the FCNC-couplings becomes very small or is simply zero. Our estimates for the 14 TeV LHC suggest that the sensitivities can be improved just a bit more to 1.1×10^{-3} with 300 fb^{-1} data.

We also note that although the sensitivities on FCNCs are better by a factor of about 1.8 for the process (c) in the $h \rightarrow 2 \text{ jets}$ detection mode compared to $h \rightarrow b\bar{b}$, due to its relatively clean signature the latter can still be quite useful to constrain the FCNCs. This, therefore confirms that it is highly desirable to tag b's for achieving better sensitivities on the FCNC couplings considered in this paper. Note also that in principle these can be further improved by a factor of two or so provided the produced top-quark and the Higgs-boson could be reconstructed fully. Therefore it is worthwhile for the ATLAS and CMS collaborations to consider possible ways of full reconstruction to further constrain the crucially important flavor-changing couplings of the Higgs-boson.

S. No.	Observable	2σ sensitivity for $\sqrt{\xi_{tc}^2 + \xi_{tu}^2}$	
(1)	Γ_t	1.3	
(2)	$\mathcal{R}_{gg\gamma\gamma}$	1.7	
(3)	$\mathcal{R}_{gg2l2\nu}$	3.3	
(4)	\mathcal{R}_{gg4l}	1.8	
(5)	(2) + (3) + (4)	1.2	
LHC-specific			
		$\sqrt{s} = 7 \text{ TeV}, \int \mathcal{L} dt = 5 \text{ fb}^{-1}$	$\sqrt{s} = 8 \text{ TeV}, \int \mathcal{L} dt = 22 \text{ fb}^{-1}$
(6)	$pp \rightarrow tt(\bar{t}\bar{t})$	0.3	0.17
(7)	$pp \rightarrow tj(\bar{t}j)$	2	1.3
(8)	$pp \rightarrow tjh(\bar{t}jh)$	1.6×10^{-3}	0.6×10^{-3}
(9)	$pp \rightarrow tt(\bar{t}\bar{t}), t \rightarrow bl\nu_l$	0.6	0.3
(10)	$pp \rightarrow tj(\bar{t}j), t \rightarrow bl\nu_l$	3.2	1.9
(11)	$pp \rightarrow tjh(\bar{t}jh), t \rightarrow bl\nu_l, h \rightarrow b\bar{b}$	7.5×10^{-3}	2.9×10^{-3}
(12)	$pp \rightarrow tjh(\bar{t}jh), t \rightarrow bl\nu_l, h \rightarrow \gamma\gamma$	11.9×10^{-2}	4.8×10^{-2}
(13)	$pp \rightarrow tjh(\bar{t}jh), t \rightarrow bl\nu_l, h \rightarrow jj$	4.2×10^{-3}	1.7×10^{-3}
(14)	(1) + (5) + (6)	0.3	0.2
(15)	(1) + (5) + (7)	0.9	0.9
(16)	(1) + (5) + (8)	1.6×10^{-3}	0.6×10^{-3}
(17)	(1) + (5) + (9)	0.6	0.3
(18)	(1) + (5) + (10)	0.9	0.9
(19)	(1) + (5) + (11)	7.5×10^{-3}	2.9×10^{-3}
(20)	(1) + (5) + (12)	11.9×10^{-2}	4.8×10^{-2}
(21)	(1) + (5) + (13)	4.2×10^{-3}	1.7×10^{-3}

Table 6: Upper bounds on the $|\xi_{tc}^2 + \xi_{tu}^2|^{1/2}$ at the 2σ level from various observations.

Acknowledgements

The work of D. A. and A. S. are supported in part by US DOE grant Nos. DE-FG02-94ER40817 (ISU) and DE-AC02-98CH10886 (BNL). The work of S. K. G. was supported in part by the *ARC Centre of Excellence for Particle*

Physics at the Tera-scale. The use of Monash University Sun Grid, a high-performance computing facility, is gratefully acknowledged. SKG would also like to thank the Regional Centre for Accelerator Based Particle Physics(RECAP) at Harish-Chandra Research Institute, Allahabad, India for providing local hospitalities during final phase of the work.

Appendix

A Composition of $pp \longrightarrow t\bar{q}_u(\bar{t}q_u)$ where $q_u = \{u, c\}$

A.1 For $\sqrt{s} = 7$ TeV

$$\begin{aligned}\sigma_{pp \rightarrow tc+t\bar{c}} &= \sigma_{cctc} + \sigma_{c\bar{c}t\bar{c}} + \sigma_{uctc} + \sigma_{u\bar{c}t\bar{c}} + \mathcal{P}_{b \rightarrow c} (\sigma_{bctb} + \sigma_{c\bar{b}t\bar{b}} + \sigma_{butb} + \sigma_{u\bar{b}t\bar{b}}) + \sigma_{b\bar{b}t\bar{c}} + \sigma_{ggt\bar{c}} \\ &= (20.83 + 0.48P_{b \rightarrow q_u})\xi_{tc}^2 + (1.26 + 6.96P_{b \rightarrow q_u})\xi_{tu}^2 \text{ fb} \\ &= 21.03\xi_{tc}^2 + 4.18\xi_{tu}^2 \text{ fb}\end{aligned}\tag{A.1}$$

$$\begin{aligned}\sigma_{pp \rightarrow \bar{t}c+\bar{t}\bar{c}} &= \sigma_{c\bar{c}\bar{t}c} + \sigma_{c\bar{c}\bar{t}\bar{c}} + \sigma_{\bar{u}c\bar{t}c} + \sigma_{\bar{u}c\bar{t}\bar{c}} + \mathcal{P}_{b \rightarrow c} (\sigma_{b\bar{c}t\bar{b}} + \sigma_{c\bar{b}t\bar{b}} + \sigma_{b\bar{u}t\bar{b}} + \sigma_{u\bar{b}t\bar{b}}) + \sigma_{b\bar{b}t\bar{c}} + \sigma_{ggt\bar{c}} \\ &= (20.83 + 0.48P_{b \rightarrow q_u})\xi_{tc}^2 + (0.2 + 1.02P_{b \rightarrow q_u})\xi_{tu}^2 \text{ fb} \\ &= 21.03\xi_{tc}^2 + 0.63\xi_{tu}^2 \text{ fb}\end{aligned}\tag{A.2}$$

$$\begin{aligned}\sigma_{pp \rightarrow tu+t\bar{u}} &= \sigma_{cutu} + \sigma_{c\bar{u}t\bar{u}} + \sigma_{uutu} + \sigma_{u\bar{u}t\bar{u}} + \mathcal{P}_{b \rightarrow u} (\sigma_{bctb} + \sigma_{c\bar{b}t\bar{b}} + \sigma_{butb} + \sigma_{u\bar{b}t\bar{b}}) + \sigma_{b\bar{b}t\bar{u}} + \sigma_{ggt\bar{u}} \\ &= (3.91 \times 10^{-6} + 0.48P_{b \rightarrow q_u})\xi_{tc}^2 + (20.6 + 6.96P_{b \rightarrow q_u})\xi_{tu}^2 \text{ fb} \\ &= 0.2\xi_{tc}^2 + 23.52\xi_{tu}^2 \text{ fb}\end{aligned}\tag{A.3}$$

$$\begin{aligned}\sigma_{pp \rightarrow \bar{t}u+\bar{t}\bar{u}} &= \sigma_{u\bar{c}\bar{t}u} + \sigma_{u\bar{c}\bar{t}\bar{u}} + \sigma_{\bar{u}u\bar{t}u} + \sigma_{\bar{u}u\bar{t}\bar{u}} + \mathcal{P}_{b \rightarrow u} (\sigma_{b\bar{c}t\bar{b}} + \sigma_{c\bar{b}t\bar{b}} + \sigma_{b\bar{u}t\bar{b}} + \sigma_{u\bar{b}t\bar{b}}) + \sigma_{b\bar{b}t\bar{u}} + \sigma_{ggt\bar{u}} \\ &= (3.91 \times 10^{-6} + 0.48P_{b \rightarrow q_u})\xi_{tc}^2 + (20.6 + 1.02P_{b \rightarrow q_u})\xi_{tu}^2 \text{ fb} \\ &= 0.2\xi_{tc}^2 + 21.03\xi_{tu}^2 \text{ fb}\end{aligned}\tag{A.4}$$

Here we have assumed $P_{b \rightarrow q_u} = 0.42$.

A.2 For $\sqrt{s} = 8$ TeV

$$\begin{aligned}\sigma_{pp \rightarrow tc+t\bar{c}} &= \sigma_{cctc} + \sigma_{c\bar{c}t\bar{c}} + \sigma_{uctc} + \sigma_{u\bar{c}t\bar{c}} + \mathcal{P}_{b \rightarrow c} (\sigma_{bctb} + \sigma_{c\bar{b}t\bar{b}} + \sigma_{butb} + \sigma_{u\bar{b}t\bar{b}}) + \sigma_{b\bar{b}t\bar{c}} + \sigma_{ggt\bar{c}} \\ &= (29.56 + 0.68P_{b \rightarrow q_u})\xi_{tc}^2 + (1.54 + 8.48P_{b \rightarrow q_u})\xi_{tu}^2 \text{ fb} \\ &= 29.85\xi_{tc}^2 + 5.1\xi_{tu}^2 \text{ fb}\end{aligned}\tag{A.5}$$

$$\begin{aligned}
\sigma_{pp \rightarrow \bar{t}c + \bar{t}\bar{c}} &= \sigma_{c\bar{c}\bar{t}c} + \sigma_{\bar{c}\bar{c}\bar{t}\bar{c}} + \sigma_{\bar{u}c\bar{t}c} + \sigma_{\bar{u}\bar{c}\bar{t}\bar{c}} + \mathcal{P}_{b \rightarrow c} (\sigma_{b\bar{c}\bar{t}b} + \sigma_{\bar{c}\bar{b}\bar{t}\bar{b}} + \sigma_{b\bar{u}\bar{t}b} + \sigma_{\bar{u}\bar{b}\bar{t}\bar{b}}) + \sigma_{b\bar{b}\bar{t}c} + \sigma_{g\bar{g}\bar{t}c} \\
&= (29.56 + 0.68P_{b \rightarrow q_u})\xi_{tc}^2 + (0.28 + 1.4P_{b \rightarrow q_u})\xi_{tu}^2 \text{ fb} \\
&= 29.85\xi_{tc}^2 + 0.34\xi_{tu}^2 \text{ fb}
\end{aligned} \tag{A.6}$$

$$\begin{aligned}
\sigma_{pp \rightarrow \bar{t}u + \bar{t}\bar{u}} &= \sigma_{cutu} + \sigma_{c\bar{u}\bar{t}\bar{u}} + \sigma_{uutu} + \sigma_{u\bar{u}\bar{t}\bar{u}} + \mathcal{P}_{b \rightarrow u} (\sigma_{b\bar{c}\bar{t}b} + \sigma_{\bar{c}\bar{b}\bar{t}\bar{b}} + \sigma_{b\bar{u}\bar{t}b} + \sigma_{\bar{u}\bar{b}\bar{t}\bar{b}}) + \sigma_{b\bar{b}\bar{t}\bar{u}} + \sigma_{g\bar{g}\bar{t}\bar{u}} \\
&= (4.89 \times 10^{-6} + 0.66P_{b \rightarrow q_u})\xi_{tc}^2 + (29.26 + 0.66P_{b \rightarrow q_u})\xi_{tu}^2 \text{ fb} \\
&= 0.32\xi_{tc}^2 + 29.54\xi_{tu}^2 \text{ fb}
\end{aligned} \tag{A.7}$$

$$\begin{aligned}
\sigma_{pp \rightarrow \bar{t}u + \bar{t}\bar{u}} &= \sigma_{u\bar{c}\bar{t}\bar{u}} + \sigma_{\bar{u}\bar{c}\bar{t}\bar{u}} + \sigma_{\bar{u}u\bar{t}\bar{u}} + \sigma_{\bar{u}\bar{u}\bar{t}\bar{u}} + \mathcal{P}_{b \rightarrow u} (\sigma_{b\bar{c}\bar{t}b} + \sigma_{\bar{c}\bar{b}\bar{t}\bar{b}} + \sigma_{b\bar{u}\bar{t}b} + \sigma_{\bar{u}\bar{b}\bar{t}\bar{b}}) + \sigma_{b\bar{b}\bar{t}\bar{u}} + \sigma_{g\bar{g}\bar{t}\bar{u}} \\
&= (4.87 \times 10^{-6} + 0.68P_{b \rightarrow q_u})\xi_{tc}^2 + (29.26 + 1.4P_{b \rightarrow q_u})\xi_{tu}^2 \text{ fb} \\
&= 0.29\xi_{tc}^2 + 30.13\xi_{tu}^2 \text{ fb}
\end{aligned} \tag{A.8}$$

References

- [1] G. Aad *et al.* [ATLAS Collaboration], Phys. Lett. B **716**, 1 (2012) [arXiv:1207.7214 [hep-ex]].
- [2] S. Chatrchyan *et al.* [CMS Collaboration], Phys. Lett. B **716**, 30 (2012) [arXiv:1207.7235 [hep-ex]].
- [3] ATLAS collaboration, ATLAS-CONF-2013-014.
- [4] CMS collaboration, CMS PAS HIG-2013-002.
- [5] K. Agashe, G. Perez and A. Soni, Phys. Rev. D **71**, 016002 (2005) [hep-ph/0408134].
- [6] K. Agashe, G. Perez and A. Soni, Phys. Rev. D **75**, 015002 (2007) [hep-ph/0606293].
- [7] M. Blanke, A. J. Buras, B. Duling, S. Gori and A. Weiler, JHEP **0903**, 001 (2009) [arXiv:0809.1073 [hep-ph]].
- [8] M. Blanke, A. J. Buras, B. Duling, K. Gemmler and S. Gori, JHEP **0903**, 108 (2009) [arXiv:0812.3803 [hep-ph]].
- [9] S. Casagrande, F. Goertz, U. Haisch, M. Neubert and T. Pfoh, JHEP **0810**, 094 (2008) [arXiv:0807.4937 [hep-ph]].
- [10] K. Agashe and R. Contino, Phys. Rev. D **80**, 075016 (2009) [arXiv:0906.1542 [hep-ph]].
- [11] A. Azatov, M. Toharia and L. Zhu, Phys. Rev. D **80**, 035016 (2009) [arXiv:0906.1990 [hep-ph]].
- [12] M. Bauer, S. Casagrande, U. Haisch and M. Neubert, JHEP **1009**, 017 (2010) [arXiv:0912.1625 [hep-ph]].

- [13] B. Keren-Zur, P. Lodone, M. Nardecchia, D. Pappadopulo, R. Rattazzi and L. Vecchi, Nucl. Phys. B **867**, 429 (2013) [arXiv:1205.5803 [hep-ph]].
- [14] T. P. Cheng and M. Sher, Phys. Rev. D **35**, 3484 (1987).
- [15] M. E. Luke and M. J. Savage, Phys. Lett. B **307**, 387 (1993) [hep-ph/9303249].
- [16] D. Atwood, L. Reina and A. Soni, Phys. Rev. D **55**, 3156 (1997) [hep-ph/9609279].
- [17] P. M. Aquino, G. Burdman and O. J. P. Eboli, Phys. Rev. Lett. **98**, 131601 (2007) [hep-ph/0612055].
- [18] N. Craig, J. A. Evans, R. Gray, M. Park, S. Somalwar, S. Thomas and M. Walker, Phys. Rev. D **86**, 075002 (2012) [arXiv:1207.6794 [hep-ph]].
- [19] K. -F. Chen, W. -S. Hou, C. Kao and M. Kohda, Phys. Lett. B **725**, 378 (2013) [arXiv:1304.8037 [hep-ph]].
- [20] C. Zhang and F. Maltoni, Phys. Rev. D **88**, 054005 (2013) [arXiv:1305.7386 [hep-ph]].
- [21] M. Jezabek and J. H. Kuhn, Nucl. Phys. B **314**, 1 (1989).
- [22] J. Beringer *et al.* [Particle Data Group Collaboration], Phys. Rev. D **86**, 010001 (2012).
- [23] A. Belyaev, N. D. Christensen and A. Pukhov, arXiv:1207.6082 [hep-ph].
- [24] D. Atwood, S. K. Gupta and A. Soni, JHEP **1304**, 035 (2013) [arXiv:1301.2250 [hep-ph]].
- [25] E. L. Berger, Q. -H. Cao, C. -R. Chen, C. S. Li and H. Zhang, Phys. Rev. Lett. **106**, 201801 (2011) [arXiv:1101.5625 [hep-ph]].
- [26] C. Degrande, J. -M. Gerard, C. Grojean, F. Maltoni and G. Servant, Phys. Lett. B **703**, 306 (2011) [arXiv:1104.1798 [hep-ph]].
- [27] J. A. Aguilar-Saavedra and M. Perez-Victoria, Phys. Lett. B **701**, 93 (2011) [arXiv:1104.1385 [hep-ph]].
- [28] S. K. Gupta, arXiv:1011.4960 [hep-ph].
- [29] Fabrice Hubaut, "*Latest ATLAS studies on Higgs to diboson states*", talk given in Moriond-2013, EW.
- [30] ATLAS collaboration, ATLAS-CONF-2013-012.
- [31] CMS collaboration, CMS PAS HIG-13-001.
- [32] C. Ochoa, "*Study of Higgs production in Bosonic Decays Channels in CMS*", talk given in Moriond-2013, QCD.
- [33] E. Mountricha, "*Study of Higgs production in Bosonic Decay Channels at ATLAS*", talk given in Moriond-2013, QCD.
- [34] ATLAS collaboration, ATLAS-CONF-2013-030.

- [35] Guillermo Gómez-Ceballos, "*Study of Standard Model Scalar Production in Bosonic Decay Channels in CMS*", talk given in Moriond-2013, EW.
- [36] CMS collaboration, CMS PAS HIG-13-003.
- [37] ATLAS collaboration, ATLAS-CONF-2013-013.
- [38] CMS collaboration, CMS PAS HIG-13-002.
- [39] M. Bona *et al.* [UTfit Collaboration], JHEP **0803**, 049 (2008) [arXiv:0707.0636 [hep-ph]].
- [40] T. Stelzer and W. F. Long, Comput. Phys. Commun. **81**, 357 (1994) [arxiv:hep-ph/9401258]; J. Alwall *et al.*, JHEP **0709**, 028 (2007) [arxiv:0706.2334 [hep-ph]]; J. Alwall *et al.*, JHEP **1106**, 128 (2011) [arxiv:1106.0522 [hep-ph]].
- [41] J. Pumplin *et al.*, JHEP **0207**, 012 (2002) [arxiv:hep-ph/0201195]; D. Stump *et al.*, JHEP **0310** 046 (2003).
- [42] ATLAS: Detector and physics performance technical design report, Volume 1, p317-346, 1999. CERN-LHCC-99-14
- [43] The ATLAS collaboration, ATLAS-CONF-2013-081.
- [44] CMS collaboration, CMS-PAS-SUS-13-002.
- [45] R. Harnik, J. Kopp and J. Zupan, arXiv:1209.1397 [hep-ph], and the references therein.